Exploring protein profiles and hub genes in ameloblastoma

SIRIMA SANGUANSIN[1], SUDAPORN KENGKARN[2], BOWORN KLONGNOI[3], SUTHIPONG CHUJAN[4,5], SITTIRAK ROYTRAKUL[6] and NAKARIN KITKUMTHORN[1]

[1]Department of Oral Biology, Faculty of Dentistry, Mahidol University, Bangkok 10400; [2]Department of Hematology, Faculty of Medical Technology, Rangsit University, Muang Pathumthani 12000; [3]Department of Oral and Maxillofacial Surgery, Faculty of Dentistry, Mahidol University, Bangkok 10400; [4]Laboratory of Pharmacology, Chulabhorn Research Institute, Bangkok 10210; [5]Center of Excellence on Environmental Health and Toxicology (EHT), Office of the Permanent Secretary (OPS), Ministry of Higher Education, Science, Research and Innovation (MHESI), Bangkok 10400; [6]Functional Proteomics Technology Laboratory, National Center for Genetic Engineering and Biotechnology, Khlong Luang, Pathumthani 12120, Thailand

Received October 2, 2023; Accepted February 9, 2024

DOI: 10.3892/br.2024.1752

Abstract. Ameloblastoma (AM) is a prominent benign odontogenic tumor characterized by aggressiveness, likely originating from tooth-generating tissue or the dental follicle (DF). However, proteomic distinctions between AM and DF remain unclear. In the present study, the aim was to identify the distinction between AM and DF in terms of their proteome and to determine the associated hub genes. Shotgun proteomics was used to compare the proteomes of seven fresh-frozen AM tissues and five DF tissues. Differentially expressed proteins (DEPs) were quantified and subsequently analyzed through Gene Ontology-based functional analysis, protein-protein interaction (PPI) analysis and hub gene identification. Among 7,550 DEPs, 520 and 216 were exclusive to AM and DF, respectively. Significant biological pathways included histone H2A monoubiquitination and actin filament-based movement in AM, as well as pro-B cell differentiation in DF. According to PPI analysis, the top-ranked upregulated hub genes were ubiquitin C (UBC), breast cancer gene 1 (BRCA1), lymphocyte cell-specific protein-tyrosine kinase (LCK), Janus kinase 1 and ATR serine/threonine kinase, whereas the top-ranked downregulated hub genes were UBC, protein kinase, DNA-activated, catalytic subunit (PRKDC), V-Myc avian myelocytomatosis viral oncogene homolog (MYC), tumor protein P53 and P21 (RAC1) activated kinase 1. When combining upregulated and downregulated genes, UBC exhibited the highest degree and betweenness values, followed by MYC, BRCA1, PRKDC, embryonic lethal, abnormal vision, Drosophila, homolog-like 1, myosin heavy chain 9, amyloid beta precursor protein, telomeric repeat binding factor 2, LCK and filamin A. In summary, these findings contributed to the knowledge on AM protein profiles, potentially aiding future research regarding AM etiopathogenesis and leading to AM prevention and treatment.

Correspondence to: Dr Nakarin Kitkumthorn, Department of Oral Biology, Faculty of Dentistry, Mahidol University, 6 Yothi Road, Ratchathewi, Bangkok 10400, Thailand
E-mail: nakarinkit@gmail.com

Key words: protein, ameloblastoma, dental follicle, liquid chromatography with tandem mass spectrometry, hub genes

Introduction

Ameloblastoma (AM) ranks among the most prevalent jaw tumors, originating in the odontogenic epithelium. It constitutes 9-11% of odontogenic tumors and 1% of all oral and maxillofacial tumors. Histologically benign, AM is slow growing but exhibits aggressive clinical behavior and a high recurrence propensity (1,2). The fifth edition of the World Health Organization Classification of Head and Neck Tumors (2022) categorizes AM as follows: Unicystic AM, conventional AM (hereafter, AM), extraosseous/peripheral AM and metastasizing AM. Additionally adenoid AM has been added in the group of benign epithelial odontogenic tumors as a new entity (2). Primarily found in the mandible (80%), AM typically occurs in individuals aged 30-40 years old (1,2). Standard treatment involves a wide surgical excision with a minimum 1 cm margin, but postsurgical challenges often lead to cosmetic and functional deformities (3). For the improvement of treatment options for AM, there is consideration for implementing precision medicine, which includes both gene and/or protein therapy. This approach aimed to tailor treatments based on the specific genetic and protein characteristics of individual patients, leading to more effective and personalized therapeutic interventions for AM. However, there was still a scarcity of molecular studies examining genetic and protein alterations in AM (3,4).

Cancer research encompassing genomics, transcriptomics and proteomics has yielded numerous breakthroughs, such as biomarker identification, molecular cancer classification and the ability to predict metastasis, treatment response and prognosis (5). Proteomics, examining the complete protein collection derived from a genome, including the isoforms, polymorphisms and post-translational modifications,

leverages high-throughput techniques, such as mass spectrometry (MS) (6). Matrix-assisted laser desorption/ionization time-of-flight (MALDI-TOF) combines a MALDI source and TOF mass analyzer. Liquid chromatography with tandem MS (LC-MS/MS), an alternate tandem MS method, is commonly used to identify proteins. LC-MS/MS utilizes electrospray ionization, whereas MALDI-TOF employs MALDI as an ionization source, with each technique featuring variable operating and performance characteristics (7,8). To the best of the authors' knowledge, data regarding tumor protein expression patterns, particularly at the proteome level, remain limited, with a limited number of studies having explored proteins associated with AM tumorigenesis (9).

The present study aimed to identify AM protein profiles via LC-MS/MS, elucidate significant protein functions and determine hub genes. Histologically, AM is considered to originate from preameloblasts during the dental follicle (DF) period in the course of tooth development (3). Therefore, the AM protein profile was compared with that of the DF. In the present study, uniformity and homogeneity were demonstrated using a three-dimensional principal component analysis (PCA) scatterplot. Subsequently, novel proteins with differential levels in AM compared with DF were identified. Both upregulated and downregulated proteins were documented, and a protein interaction network was constructed. Ultimately, the insights gained from the hub genes contributed to an enhanced understanding of AM pathogenesis and may have clinical implications.

Materials and methods

Sample recruitment. A total of seven fresh-frozen AM tissues and five DF tissues were included in the present study. AM tissues were obtained during mandibulectomy from patients with AM (age range, 13-66 years; sex, female: male, 4:3), whereas DF tissues were obtained from patients who underwent wisdom tooth extraction (age range, 17-25 years; sex, female: male, 3:2). The Department of Oral and Maxillofacial Surgery, Faculty of Dentistry, Mahidol University, Bangkok, Thailand, served as the collection site from April 2021 to February 2022. The present study included AM samples with at least 80% tumor content, while cases with poor-quality DNA were excluded in the investigations. Specimens were halved, with one part undergoing histopathological confirmation. The demographic information for each sample is shown in Table SI. The present study was approved by the Institutional Review Board of the Faculty of Dentistry/Faculty of Pharmacology, Mahidol University, Bangkok, Thailand (approval no. COA.NO.MU-DT/PY-IRB 2021/034.3003) and was conducted in accordance with the Declaration of Helsinki (1975), as revised in 2013. Written informed consent was obtained from all patients.

Protein preparation for proteomics analysis. The frozen tissue, sized at 0.5x0.5x0.5 cm^3, was collected at -80˚C and stored in a 1.5-ml tube. Subsequently, the tissue was ground in liquid nitrogen using an Axygen™ Tissue Grinder (Thermo Fisher Scientific, Inc.) and then solubilized using liquid nitrogen and detergent lysis [50 mM Tris-HCl (pH 7.2), 1% sodium dodecyl sulfate (SDS) and 20 mM dithiothreitol (DTT)], with mixing at room temperature for 10 min. Following sonication for 5 sec twice (80% amplitude), the lysed tissue was heated at 72˚C for 3 min before undergoing centrifugation at 12,000 x g for 30 min. Protein solutions were stored at -20˚C until analysis.

Gel-free digestion for proteomics analysis. Total protein pellets (3 g) were mixed with an MS analysis lysis buffer [0.1% RapidGest SF (Waters Corporation) in 20 mM ammonium bicarbonate]. Sulfhydryl bonds were reduced with 10 mM DTT in a 10-mM ammonium bicarbonate solution via heating at 60˚C for 1 h, followed by alkylation of sulfhydryl groups with 100 mM iodoacetamide in a 10-mM ammonium bicarbonate solution at room temperature for 45 min in a light-protected environment. After cleaning with Zeba Spin Desalting Columns (MilliporeSigma), digestion was performed by adding 50 ng/μl sequencing-grade trypsin (1:20; Promega Corporation) to the solution and incubating at 37˚C for 6 h. Tryptic peptides were dried at 44˚C under vacuum conditions, protonated with 0.1% formic acid and injected into the LC-MS/MS system (as described in the following section).

Label-free proteomic quantification via LC-MS/MS. Tryptic peptides were analyzed using an Ultimate 3000 Nano/Capillary LC System (Thermo Fisher Scientific, Inc.), coupled with a Hybrid Quadrupole Q-TOF Impact II™ (Bruker Daltonics; Bruker Corporation) equipped with a nano-captive spray ion source. Extracted peptides (500 ng) were added to the trapping column (PepMap100, C18, 300; Thermo Fisher Scientific, Inc.). At a column temperature of 60˚C, the sample was resolved on an analytical column (PepSwift C18 Nano Column, 100 m x15 cm). To elute peptides into the mass spectrometer, a linear gradient elution method with a gradual increase in mobile phases A and B at a steady flow rate of 0.35 l/min was used. Mobile phase A comprised water with 0.1% formic acid, whereas mobile phase B comprised 80% acetonitrile with 0.1% formic acid. The mobile phase gradients were conditioned as follows: i) Equilibration period, 0-4.0 min: 10% phase B; ii) separation period, 4.01-30.0 min: 10-60% phase B; iii) washing period, 30.01-40.00 min: 95% phase B; and iv) re-equilibration period, 40.01-50.00 min: 10% phase B. Electrospray ionization using CaptiveSpray was performed at 1.6 kV. MS and MS/MS spectra were fully collected in positive-ion mode (m/z=400-2,200), maintaining a mass accuracy within 1.6 parts per million (ppm) after tuning and internal calibration with sodium trifluoroacetate. LC-MS/MS spectra were collected using a data-dependent auto-MS/MS technique with a 3-sec cycle duration.

Proteomic data interpretation. Raw LC-MS/MS spectra were converted to mzXML format using CompassXport (v.3.0.9.2; Bruker Daltonics; Bruker Corporation). DeCyder MS 2.0 was employed to evaluate the mzXML format of LC-MS/MS datasets for label-free peptide quantification using the MS spectra profile (GE Healthcare). To determine the relative amount, peak volumes and charge states of the same peptide from different LC-MS runs using PepMatch modules version 0.7.8 (https://pypi.org/project/pepmatch/0.7.8/). Data processing followed specific criteria: Allowing three missed cleavages, setting a 20-ppm peptide mass tolerance for the primary search, using trypsin as the digesting enzyme, applying carbamidomethylation to cysteine as a fixed modification and considering oxidation of methionine

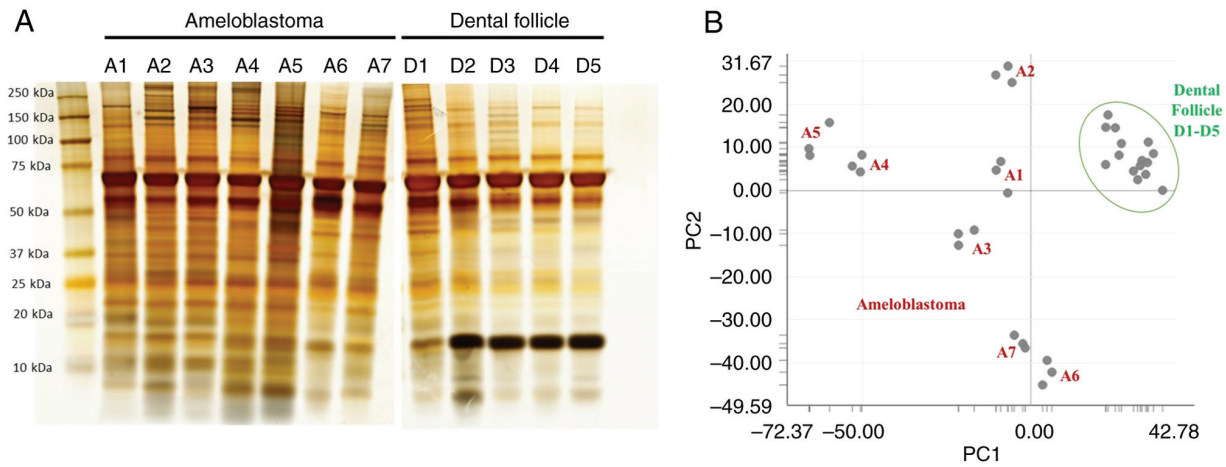

Figure 1. Differential distribution of AM and DF. (A) Gel-based fractionation SDS-PAGE of 4-20% gradient Bis-Tris. (B) Principal component analysis plot of AM and DF. AM, ameloblastoma; DF, dental follicle.

and acetylation of the protein N-terminus as variable modifications. The selected protein was identified using Mascot (v. 2.3.02; Matrix Science, Ltd.).

Differentially expressed proteins (DEPs). Information regarding particular proteins was annotated using UniProtKB/Swiss-Prot entries (http://www.uniprot.org). Enrichr software (https://amp.pharm.mssm.edu/Enrichr/) was used to conduct gene list enrichment analysis (10). DEPs in AM or DF tissue were identified and analyzed. Proteins specific to AM were termed 'upregulated proteins', whereas those exclusive to DF were labeled 'downregulated proteins'.

Gene Ontology (GO) and pathway enrichment analyses. Freely accessible databases, namely the Database for Annotation, Visualization, and Integrated Discovery (DAVID; http://david.ncifcrf.gov/home.jsp) and the Kyoto Encyclopedia of Genes and Genomes (KEGG), provided biological data and analysis tools (https://www.genome.jp/kegg/pathway.html). DAVID was used for GO (11) and KEGG pathway enrichment analyses of differentially expressed genes (DEGs). Biological process (BP), cellular component (CC) and molecular function (MF) GO terms, as well as significant pathways associated with DEGs, were identified. A threshold of $P<0.05$ was used to determine statistical significance.

Protein-protein interaction (PPI) network construction and hub gene identification. NetworkAnalyst (https://www.networkanalyst.ca/), a free web-based tool for visualizing statistical meta-analysis, data mining and construction of biological networks, facilitated gene list meta-analysis (12). Biological data integration was achieved using robust statistical procedures and the data were visualized using PPI networks. In the present study, the Search Tool for Retrieval of Interacting Genes/Proteins (STRING) software version 11 (https://string-db.org/cgi/input.pl) was selected as a PPI database (13), requiring experimental evidence and a high confidence (900) cut-off score for reliable results. The number of proteins interacting with a node determined node importance. The top 10% of nodes by degree value were selected for potential physiological regulatory functions.

Statistical analysis. Individual samples were performed by LC-MS/MS in triplicate. The maximum score was applied to the protein score of each sample. Principal component analysis (PCA) was executed with the software ClinProTools 2.2. (Bruker Deltonik GmbH). Regarding DEPs, the number of unique proteins identified in each AM or DF group was recorded. An unpaired t-test was applied to identify DEPs and Fisher's exact test was used to assess for enrichment in GO terms and KEGG pathways. False discovery rate adjusted ($P<0.05$) was considered to indicate a statistically significant GO and KEGG pathway (11).

Results

Protein profile and analyses of DEPs. The AM (A1-A7) and DF (D1-D5) groups were isolated and further divided into two fractions. The first fraction was subjected to gel-based fractionation (4-20% gradient Bis-Tris SDS-polyacrylamide gel electrophoresis) to observe and compare protein profiles and the other fraction was subjected to LC-MS/MS to quantify DEPs. Gel-based protein extraction revealed distinct patterns between AM and DF protein profiles. Although both exhibited a similar 25-75 kDa range, the DF group displayed higher density in the 10-20 kDa range compared with the AM group (Fig. 1A). PCA reduced the data dimensionality to facilitate visualization and interpretation (Fig. 1B). Notably, the protein patterns differed between the AM and DF groups across various protein sizes, suggesting that these proteins play crucial roles in biological mechanisms with regard to function in tumor development, leading to substantial changes in protein abundance.

In addition to gel-based fractionation, gel-free proteomics is a highly sensitive method for protein identification and quantification. LC-MS/MS spectra from the LC runs were predominantly identified using the UniProt database, revealing 7,550 DEPs. According to the Venn diagram, the accounted proteins were those that were specific to each group, including 520 for AM and 216 for DF (Fig. 2). The uppermost 30 genes that were the most distinctive are presented in Table I. In AM, uncharacterized protein C7orf45 (CG045), 5-hydroxytryptamine receptor 5B, pseudogene (HTR5B), protein FAM47A

Table I. The 30 most unique and highest upregulated genes in AM and DF.

Upregulated genes in AM			Upregulated genes in DF		
Protein symbol	Protein description	Score	Protein symbol	Protein description	Score
CG045	Uncharacterized protein C7orf45	21.85	EDEM2	ER degradation-enhancingalpha-mannosidase-like protein 2	19.50
HTR5B	5-hydroxytryptamine receptor 5B, pseudogene	21.00	ADAP1	Arf-GAP with dual PHdomain-containing protein 1	18.72
FA47A	Protein FAM47A	20.61	ANGL2	Angiopoietin-related protein 2	18.63
ZN408	Zinc finger protein 408	20.27	SETD5	Histone-lysine N-methyltransferase SETD5	18.52
SHRM4	Protein Shroom4	19.99	ARH40	Rho guanine nucleotide exchange factor 40	17.60
DPYL3	Dihydropyrimidinase-related protein 3	19.47	BTBD9	BTB/POZ domain-containing protein 9	17.20
BAZ2B	Bromodomain adjacent to zinc finger domain protein 2B	18.94	DYN1	Dynamin-1	16.69
ZFHX3	Zinc finger homeobox protein 3	18.34	RPC3	DNA-directed RNA polymerase III subunit RPC3	16.67
LAR1B	La-related protein 1B	18.18	PRKDC	DNA-dependent protein kinase catalytic subunit	16.57
CARD6	Caspase recruitment domain-containing protein 6	18.15	CHP2	Calcineurin B homologous protein 2	16.47
ACM5	Muscarinic acetylcholine receptor M5	17.65	E41LB	Band 4.1-like protein 4B	16.17
CCD83	Coiled-coil domain-containing protein 83	17.58	CE290	Centrosomal protein of 290 kDa	16.14
MMEL1	Membrane metallo-endopeptidase-like 1	17.37	LEUK	Leukosialin	16.01
GMEB1	Glucocorticoid modulatory element-binding protein 1	17.24	SRRM2	Serine/arginine repetitive matrix protein 2	16.00
HPLN1	Hyaluronan and proteoglycan link protein 1	17.19	MYC	Myc proto-oncogene protein	15.97
SPAT5	Spermatogenesis-associated protein 5	17.05	A2AP	Alpha-2-antiplasmin	15.85
CH073	Putative uncharacterized protein C8orf73	17.02	MYO6	Unconventional myosin-VI	15.75
RLA0L	60S acidic ribosomal protein P0-like	16.99	BARX2	Homeobox protein BarH-like 2	15.52
GBP3	Guanylate-binding protein 3	16.94	TLK1	Serine/threonine-protein kinase tousled-like 1	15.50
RH10L	Rho GTPase-activating protein 10-like	16.90	DYH1	Dynein heavy chain 1, axonemal	15.47
PATE1	Prostate and testis expressed protein 1	16.89	RXLT1	Ribitol-5-phosphate xylosyl-transferase 1	15.39
B4GN4	Beta-N-acetylgalactosaminyltransferase 1	16.88	DLG5	Disks large homolog 5	15.32
KS6C1	Ribosomal protein S6 kinase delta-1	16.87	NFU1	NFU1 iron-sulfur cluster scaffold homolog, mitochondrial	15.21
MN1	Probable tumor suppressor protein MN1	16.84	IGSF3	Immunoglobulin superfamily member 3	15.17
LYAG	Lysosomal alpha-glucosidase	16.74	PRP18	Pre-mRNA-splicing factor 18	15.14
ATPA	ATP synthase subunit alpha, mitochondrial	16.70	RHG30	Rho GTPase-activating protein 30	15.06
ZN606	Zinc finger protein 606	16.70	SRSF9	Serine/arginine-rich splicing factor 9	15.04
CELR3	Cadherin EGF LAG seven-pass G-type receptor 3	16.68	ITPR2	Inositol 1,4,5-trisphosphate receptor type 2	15.03
BRSK2	BR serine/threonine-protein kinase 2	16.63	GDN	Glia-derived nexin	15.02
NR1D2	Nuclear receptor subfamily 1 group D member 2	16.60	FNBP1	Formin-binding protein 1	14.99

Table II. GO terms of upregulated genes.

Term	Description	P-value
A, Biological process		
GO:0035518	Histone H2A monoubiquitination	0.0071
GO:0030048	Actin filament-based movement	0.0071
GO:0007169	Transmembrane receptor protein tyrosine kinase signaling pathway	0.0078
GO:0061178	Regulation of insulin secretion involved in cellular response to glucose stimulus	0.0086
GO:0050885	Neuromuscular process controlling balance	0.0162
GO:0031572	G2 DNA damage checkpoint	0.0203
GO:0001764	Neuron migration	0.0206
GO:0007411	Axon guidance	0.0233
GO:0000226	Microtubule cytoskeleton organization	0.0288
GO:0035556	Intracellular signal transduction	0.0318
B, Cellular component		
GO:0008076	Voltage-gated potassium channel complex	$6.96x10^{-4}$
GO:0005856	Cytoskeleton	0.0013
GO:0005737	Cytoplasm	0.0018
GO:0033268	Node of Ranvier	0.0040
GO:0005634	Nucleus	0.0277
GO:0000794	Condensed nuclear chromosome	0.0317
GO:0005730	Nucleolus	0.0332
GO:0031252	Cell leading edge	0.0343
GO:0097513	Myosin II filament	0.0362
GO:0016589	NURF complex	0.0711
C, Molecular function		
GO:0005524	ATP binding	$1.43x10^{-4}$
GO:0005516	Calmodulin binding	0.0059
GO:0003779	Actin binding	0.0115
GO:0016874	Ligase activity	0.0123
GO:0004674	Protein serine/threonine kinase activity	0.0142
GO:0001948	Glycoprotein binding	0.0215
GO:0005251	Delayed rectifier potassium channel activity	0.0467
GO:0071558	Histone demethylase activity (H3-K27 specific)	0.0605
GO:0030898	Actin-dependent ATPase activity	0.0605
GO:0044822	Poly(A) RNA binding	0.0643
D, KEGG pathway		
cfa04611	Platelet activation	0.0018
cfa04015	Rap1 signaling pathway	0.0186
cfa04915	Estrogen signaling pathway	0.0746
cfa03460	Fanconi anemia pathway	0.0922
cfa04114	Oocyte meiosis	0.0980

GO, Gene Ontology; KEGG, Kyoto Encyclopedia of Genes and Genomes.

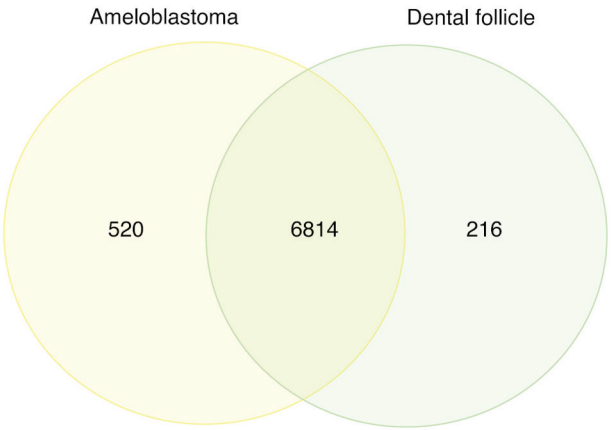

Figure 2. Venn diagram demonstrated 520 proteins that are unique to ameloblastoma and 216 proteins that are specific to dental follicle.

(FA47A), Zinc finger protein 408 (ZN408) and protein Shroom4 (SHRM4) achieved the greatest scores. Conversely, in DF, ER degradation-enhancing alpha-mannosidase-like protein 2 (EDEM2), Arf-GAP with dual PH domain-containing protein 1 (ADAP1), angiopoietin-related protein 2 (ANGL2), histone-lysine N-methyltransferase SETD5 (SETD5) and Rho guanine nucleotide exchange factor 40 (ARH40) exhibited the highest scores.

GO term and KEGG pathway enrichment analyses of DEGs. To comprehend the biological functions of the identified DEGs, GO term and KEGG pathway enrichment analyses using DAVID were conducted. The top ten distinctive findings pertaining to BP, CC and MF specific to AM are highlighted in Table II. Notably, the most enriched genes were associated with 'histone H2A monoubiquitination' (BP), 'actin filament-based movement' (BP), 'voltage-gated potassium channel complex' (CC) and 'ATP-binding' (MF). The downregulated GO terms in AM, primarily involving 'pro-B cell differentiation' (BP), 'cytoplasm' (CC), 'ATP-binding' (MF) and 'poly(A) RNA binding' are presented in Table III.

Enrichment analysis of KEGG pathways unveiled an overrepresentation of specific pathways related to upregulated genes. 'Platelet activation' emerged as the most significant pathway, followed by the 'Rap1 signaling pathway', the 'estrogen signaling pathway', the 'Fanconi anemia pathway' and 'oocyte meiosis' (Table II). Conversely, downregulated genes were mainly involved in 'proteoglycans in cancer' and 'the glucagon signaling pathway', as indicated in Table III.

PPI network construction and hub gene identification. NetworkAnalyst was used to establish and visualize the PPI network, employing a minimum network approach to simplify and focus on core protein associations (12). This approach retained seed proteins and essential non-seed proteins, allowing the study of the key interactions among these proteins. A degree of >20 was set as the cut-off criterion. The upregulated genes included 305 nodes, 825 edges and 178 seeds. The top ten proteins in the PPI network of these genes were ubiquitin C (UBC), breast cancer gene 1 (BRCA1), lymphocyte cell-specific protein-tyrosine kinase (LCK), Janus kinase 1 (JAK1), ATR serine/threonine kinase (ATR), structural maintenance of chromosomes 3 (SMC3), regulatory associated protein of MTOR complex 1 (RPTOR), cell division cycle 27 (CDC27), phospholipase C beta 3 (PLCB3) and vasodilator stimulated phosphoprotein (VASP) (Fig. 3). The PPI network of downregulated genes comprised 113 nodes, 256 edges and 75 seeds. The top five proteins in this network, UBC, protein kinase, DNA-activated, catalytic subunit (PRKDC), V-Myc avian myelocytomatosis viral oncogene homolog (MYC), tumor protein P53 (TP53) and P21 (RAC1) activated kinase 1 (PAK1), were considered hub genes for downregulated DEGs (Fig. 4). Combining upregulated and downregulated genes in a PPI network resulted in 434 nodes, 1,457 edges and 254 seeds. As revealed in Table IV and Fig. 5, UBC exhibited the highest degree and betweenness values in this network, followed by MYC, BRCA1, PRKDC, embryonic lethal, abnormal vision, Drosophila, homolog-like 1 (ELAVL1), myosin heavy chain 9 (MYH9), amyloid beta precursor protein (APP), telomeric repeat binding factor 2 (TERF2), LCK and filamin A (FLNA).

Table III. GO terms of downregulated genes.

Term	Description	P-value
A, Biological process		
GO:0002328	Pro-B cell differentiation	0.0157
GO:0007018	Microtubule-based movement	0.0423
B, Cellular process		
GO:0005737	Cytoplasm	0.0070
GO:0005730	Nucleolus	0.0198
GO:0015629	Actin cytoskeleton	0.0249
GO:0016020	Membrane	0.0623
C, Molecular function		
GO:0005524	ATP binding	0.0028
GO:0044822	Poly(A) RNA binding	0.0095
GO:0051536	Iron-sulfur cluster binding	0.0374
GO:0003777	Microtubule motor activity	0.0394
D, KEGG pathway		
cfa05205	Proteoglycans in cancer	0.0687
cfa04922	Glucagon signaling pathway	0.0810

GO, Gene Ontology; KEGG, Kyoto Encyclopedia of Genes and Genomes.

Discussion

Through the present study, the identification of unique protein patterns between AM and DF, which may have been engaged in the process of transforming from DF to AM at the scale of proteins, was achieved. Changes in biological processes and

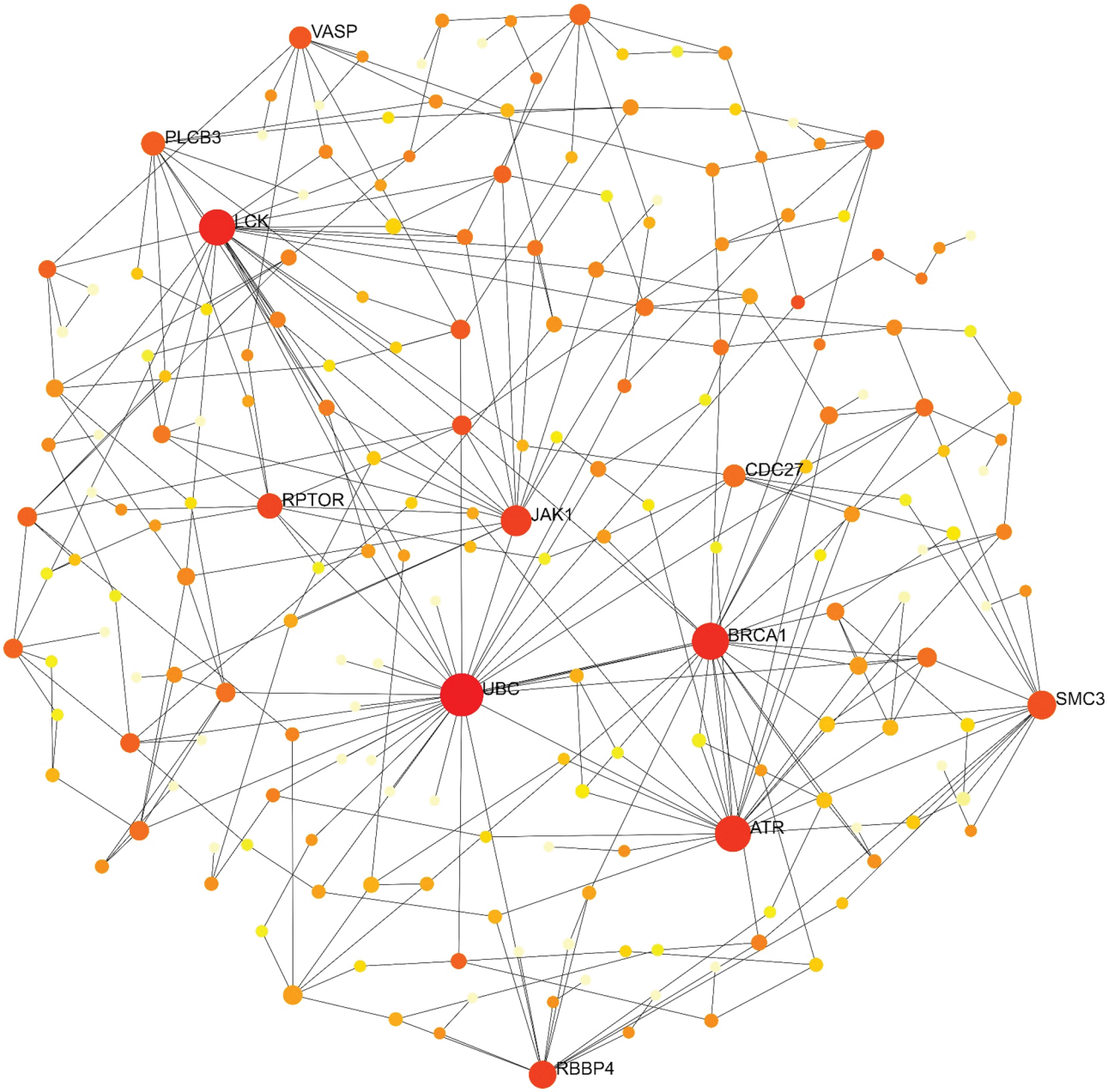

Figure 3. Protein-protein interaction network of upregulated genes revealed ten hub genes (red circles).

major signaling transductions that play crucial roles in AM were also investigated. These observations were based on the protein patterns that were analyzed.

The biological function analysis findings highlighted upregulation of H2A monoubiquitination and actin filament-based movement in AM. H2A monoubiquitination, a key histone modification, occurs when a particular lysine residue in the core histone protein H2A is taken by a single ubiquitin molecule. This process is crucial for regulating gene expression and chromatin structure, affecting DNA packaging and gene accessibility to transcription factors and regulatory proteins (14,15). To the best of the authors' knowledge, the role of H2A monoubiquitination in AM has not been explored. However, similar to other tumors, it may play a role in governing oncogene and tumor suppressor gene expression via chromatin access, as well as guiding their cellular differentiation from DF (16).

Actin filaments are essential components of the cell cytoskeleton, playing a key role in cellular processes such as motility. They are essential for functions such as cell migration, muscle contraction, cytokinesis and cell division (17). Although actin filaments and cell motility are fundamental processes in biology, they are not directly linked to AM formation or development (18). The invasive behavior of AM, infiltrating healthy tissues, is a distinctive feature contributing to its progression (3). Changes in tumor cell adhesion molecules may contribute to invasiveness, influencing tumor growth and tissue invasion (19). Among these changes, the loss or dysregulation of different cell adhesion molecules is significant because the biological processes underlying odontogenic tumors depend on cell adhesion (20). However, additional investigation of these pathway changes at the molecular level of AM development and progression must be further explored.

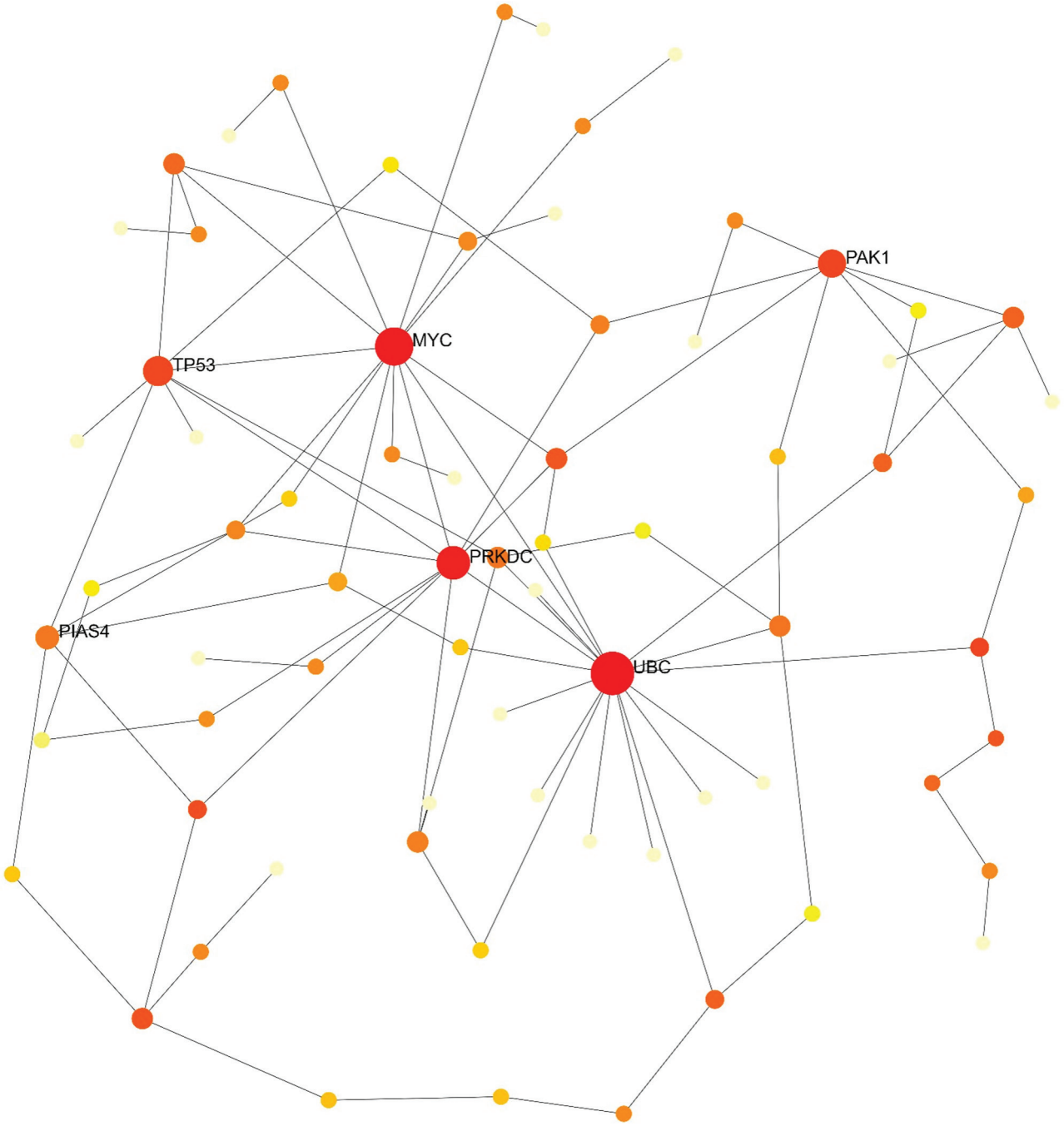

Figure 4. Protein-protein interaction network of downregulated genes revealed six hub genes (red circles).

Pathway enrichment analysis identified 'platelet activation' and the 'Rap1 signaling pathway' as the top-ranked pathways associated with AM-upregulated proteins. Platelet activation is an important part of hemostasis and thrombosis. Activated platelets stick to sites of vascular damage to form blood clots, which stop excessive bleeding (21). A prior study indicated higher expression of platelet-derived endothelial cell growth factor/thymidine phosphorylase (PD-ECGF/TP) in AM compared with the DF (22). In addition, PD-ECGF/TP reactivity was observed in granular cell AM (23), which suggested that it is involved in both tumor and normal cells. This indicated that angiogenic factors play a part in the development of ameloblasts.

The Rap1 signaling pathway regulates cell adhesion, proliferation and migration. Specifically, it regulates integrins and cadherins, promoting cell-cell and extracellular matrix adhesion (24). In the context of tumor invasion and metastasis, matrix metalloproteinases (MMPs) break down extracellular matrix barriers, cleave and activate specific target proteins, and influence cell adhesion processes. In head and neck squamous cell carcinoma, it was revealed that Rap1 involvement in promoting β-catenin nuclear localization triggered T-cell factor-dependent transcription of MMP7, contributing to tumor cell invasion (25). Although Rap1 signaling is a pivotal pathway implicated in various diseases, its specific association with AM has not been documented, necessitating further study of Rap1 signaling mechanisms.

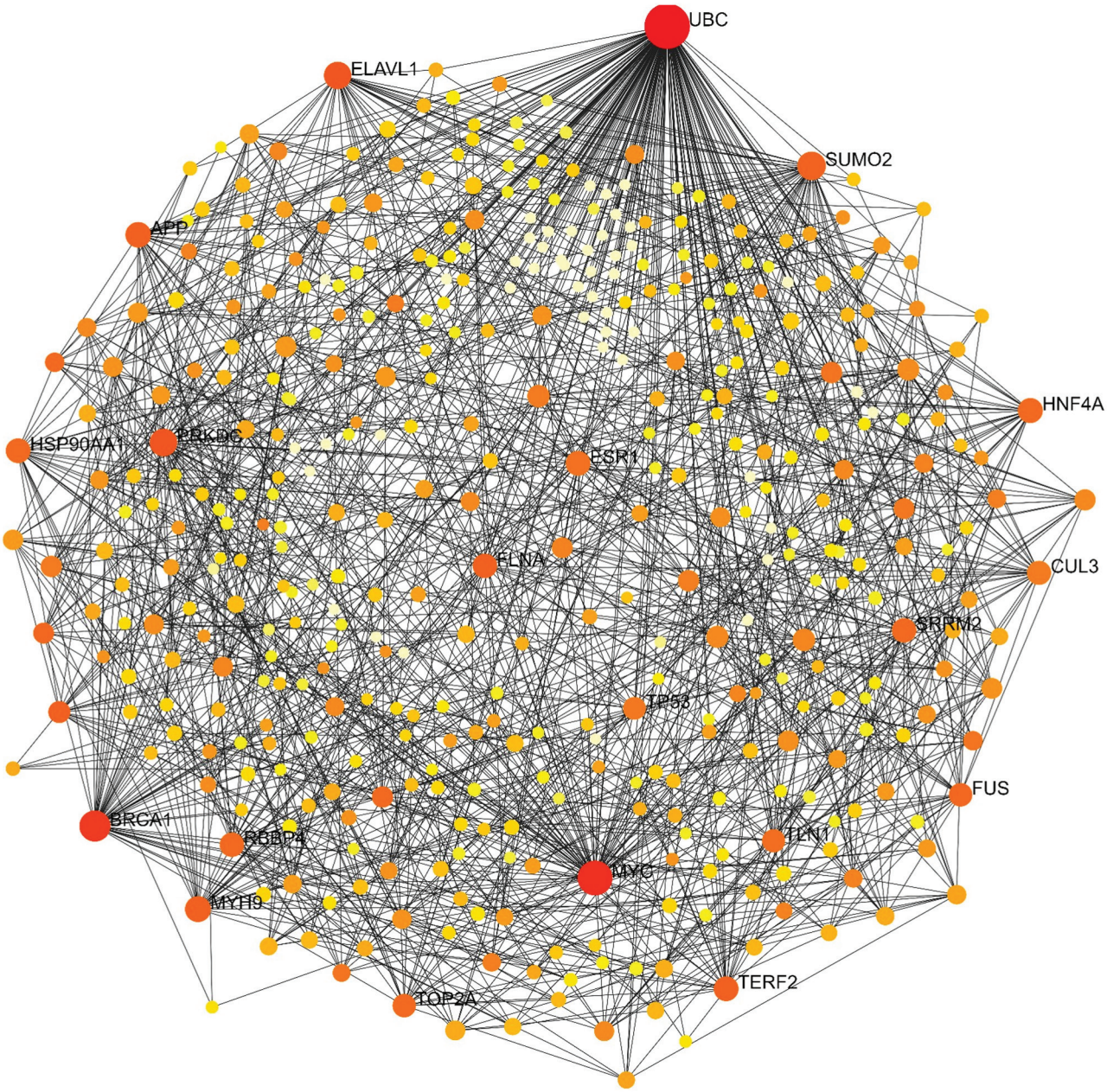

Figure 5. Protein-protein interaction network of the combination of upregulated and downregulated genes revealed six hub genes (red circles).

It was determined that the prominent pathway associated with downregulated genes in AM involves proteoglycans. Proteoglycans, comprising a core protein and lengthy carbohydrate chains known as glycosaminoglycans, play a crucial role in the extracellular matrix. They provide structural support and regulate cellular behavior (26). By interacting with growth factors, cytokines and signaling molecules, proteoglycans influence cell proliferation, migration and differentiation (27). Alterations in the extracellular matrix, including changes in proteoglycans, have significant implications for tumor progression, invasion and metastasis in cancer. However, the specific roles of proteoglycans can vary substantially in different cancer types (28). Proteoglycans also contribute significantly to odontogenesis, as evidenced by their involvement in cell differentiation stages during human and animal tooth development models (29). Some proteoglycan genes, initially silenced during tooth development, reactivate in some odontogenic tumors (30). This reactivation is associated with tumor-related processes such as growth, invasion and the loss of cell adhesion, highlighting the role of proteoglycans in tumorigenesis (31). In summary, the proteoglycan pathway appears to be crucial in the etiology of AM.

The term 'hub gene' refers to a gene that holds a central position in a biological network or system (32). In molecular biology and genetics, it typically signifies a gene with numerous connections or interactions within a pathway or network. Hub genes provide valuable insights into the molecular mechanisms associated with cancer development, progression and treatment response (32,33). In the present study, UBC and MYC were identified as hub genes with the highest degree values. Exploring their roles in AM could unveil potential therapeutic

Table IV. Top ten gene interactions (betweenness level) of significant genes.

Gene name	Symbol	Degree	Betweeness
Ubiquitin C	UBC	193	50,842.56
V-Myc avian myelocytomatosis viral oncogene homolog	MYC	79	12,828.16
Breast cancer gene 1	BRCA1	55	8,345.05
Protein kinase, DNA-activated, catalytic subunit	PRKDC	38	3,207.52
Embryonic lethal, abnormal vision, Drosophila, homolog-like 1	ELAVL1	37	3,194.60
Myosin heavy chain 9	MYH9	31	2,438.32
Amyloid beta precursor protein	APP	30	2,370.31
Telomeric repeat binding factor 2	TERF2	27	2,346.16
Lymphocyte cell-specific protein-tyrosine kinase	LCK	19	2,241.01
Filamin A	FLNA	26	2,232.92

targets and guide the development of personalized treatment strategies.

The UBC gene encodes ubiquitin C and has emerged as the top-ranked hub gene from the PPI network analysis. Ubiquitin acts as either an oncogene or a tumor suppressor gene in various cancers and is involved in crucial cellular processes such as protein localization, the cell cycle, transcription, DNA damage repair and endocytosis (34). In tumors, the P53 protein is primarily located in the nucleoplasm, where it binds specifically to DNA. It facilitates gene repair and undergoes post-translational changes, including phosphorylation, acetylation, methylation and ubiquitination (35). While the specific role of UBC in AM has not been reported, the findings of the present study indicated that UBC may potentially contribute to the disease, underscoring the importance of further exploration into the associated mechanisms of this gene.

In the PPI network analysis, MYC was identified as a key hub gene. Notably, c-MYC plays a role in promoting oncogene-induced senescence, a critical process in tumor suppressor mechanisms that helps prevent cell transformation (36). Previous research has established a connection between telomerase activity and both oncogenesis and odontogenic epithelial proliferation. Additionally, there is evidence suggesting that the c-MYC protein may act as a regulator of telomerase activity in AM (37).

One limitation of this research lies in the assessment of a limited number of patients. A study conducted across multiple centers or recruiting a substantial number of participants would yield a greater quantity of data and higher-quality results. Another limitation is the potential exclusion of proteins with low abundance or hydrophilic properties from the results. LCMS/MS with electrospray ionization generates multiple-charged ions, leading to the loss of single-charged ions (38). Consequently, certain proteins with low abundance may be omitted from the protein records. One notable example is BRAF V600E, which is currently recognized for its role in mandibular AM tumorigenesis (39,40).

In summary, through the PPI network analysis, novel hub genes associated with AM were discovered. Notably, UBC, BRCA1, LCK, JAK1, ATR, PRKDC, MYC, TP53 and PAK1 were identified as common hub genes. The critical biological pathways involved in AM were 'histone H2A monoubiquitination' and 'actin filament-based movement'. Further investigation into these essential hub genes and pathways is necessary in order to facilitate the development of practical applications that will be of assistance in the treatment of individuals afflicted with AM.

Acknowledgements

The authors would like to express their gratitude to the Functional Proteomics Technology Laboratory, National Center for Genetic Engineering and Biotechnology (Pathumthani, Thailand) for providing the facilities and laboratory equipment.

Funding

The present study was supported by Mahidol University, Faculty of Dentistry Grant (grant no. DTRS-EG-2021-04).

Availability of data and materials

The datasets used and/or analyzed during the current study are available from the corresponding author on reasonable request.

Authors' contributions

SS and NK conceived the study, designed the experiments, confirm the authenticity of all the raw data, analyzed the data and wrote the manuscript. SS, SK, SC and SR performed experiments and interpreted data. NK and BK recruited the patients and collected the clinical samples. All authors have read and approved the final version of the manuscript.

Ethics approval and consent to participate

The present study was approved by the Institutional Review Board of the Faculty of Dentistry/Faculty of Pharmacology, Mahidol University, Bangkok, Thailand (approval no. COA. NO.MU-DT/PY-IRB 2021/034.3003) and was conducted in accordance with the Declaration of Helsinki (1975), as revised in 2013. Written informed consent was obtained from all patients.

Patient consent for publication

Not applicable.

Competing interests

The authors declare that they have no competing interests.

References

1. Ghai S: Ameloblastoma: An updated narrative review of an enigmatic tumor. Cureus 14: e27734, 2022.
2. Vered M and Wright JM: Update from the 5th edition of the World Health Organization classification of head and neck tumors: Odontogenic and maxillofacial bone tumours. Head Neck Pathol 16: 63-75, 2022.
3. Effiom OA, Ogundana OM, Akinshipo AO and Akintoye SO: Ameloblastoma: Current etiopathological concepts and management. Oral Dis 24: 307-316, 2018.
4. Brown NA and Betz BL: Ameloblastoma: A review of recent molecular pathogenetic discoveries. Biomark Cancer 7 (Suppl 2): S19-S24, 2015.
5. Chakraborty S, Hosen MI, Ahmed M and Shekhar HU: Onco-multi-OMICS approach: A new frontier in cancer research. Biomed Res Int 2018: 9836256, 2018.
6. Sallam RM: Proteomics in cancer biomarkers discovery: Challenges and applications. Dis Markers 2015: 321370, 2015.
7. Fernández-Puente P, Mateos J, Blanco FJ and Ruiz-Romero C: LC-MALDI-TOF/TOF for shotgun proteomics. Methods Mol Biol 1156: 27-38, 2014.
8. Darie-Ion L, Whitham D, Jayathirtha M, Rai Y, Neagu AN, Darie CC and Petre BA: Applications of MALDI-MS/MS-based proteomics in biomedical research. Molecules 27: 6196, 2022.
9. Cui Y, Li H, Xiao T, Zhang X, Hou Y, Li H and Li X: A proteomics study to explore differential proteins associated with the pathogenesis of ameloblastoma. J Oral Pathol Med 52: 528-538, 2023.
10. Kuleshov MV, Jones MR, Rouillard AD, Fernandez NF, Duan Q, Wang Z, Koplev S, Jenkins SL, Jagodnik KM, Lachmann A, *et al*: Enrichr: A comprehensive gene set enrichment analysis web server 2016 update. Nucleic Acids Res 44 (W1): W90-W97, 2016.
11. Harris MA, Clark J, Ireland A, Lomax J, Ashburner M, Foulger R, Eilbeck K, Lewis S, Marshall B, Mungall C, *et al*: The gene ontology (GO) database and informatics resource. Nucleic Acids Res 32 (Database Issue): D258-D261, 2004.
12. Zhou G, Soufan O, Ewald J, Hancock REW, Basu N and Xia J: NetworkAnalyst 3.0: A visual analytics platform for comprehensive gene expression profiling and meta-analysis. Nucleic Acids Res 47 (W1): W234-W241, 2019.
13. Szklarczyk D, Gable AL, Lyon D, Junge A, Wyder S, Huerta-Cepas J, Simonovic M, Doncheva NT, Morris JH, Bork P, *et al*: STRING v11: Protein-protein association networks with increased coverage, supporting functional discovery in genome-wide experimental datasets. Nucleic Acids Res 47 (D1): D607-D613, 2019.
14. Zhang Y, Sun Z, Jia J, Du T, Zhang N, Tang Y, Fang Y and Fang D: Overview of histone modification. Adv Exp Med Biol 1283: 1-16, 2021.
15. Cao J and Yan Q: Histone ubiquitination and deubiquitination in transcription, DNA damage response, and cancer. Front Oncol 2: 26, 2012.
16. Guo XE, Ngo B, Modrek AS and Lee WH: Targeting tumor suppressor networks for cancer therapeutics. Curr Drug Targets 15: 2-16, 2014.
17. Tang DD and Gerlach BD: The roles and regulation of the actin cytoskeleton, intermediate filaments and microtubules in smooth muscle cell migration. Respir Res 18: 54, 2017.
18. Nishikawa S: Cytoskeleton, intercellular junctions, planar cell polarity, and cell movement in amelogenesis. J Oral Biosci 59: 197-204, 2017.
19. Kiefel H, Bondong S, Hazin J, Ridinger J, Schirmer U, Riedle S and Altevogt P: L1CAM: A major driver for tumor cell invasion and motility. Cell Adh Migr 6: 374-384, 2012.
20. Nagi R, Sahu S and Rakesh N: Molecular and genetic aspects in the etiopathogenesis of ameloblastoma: An update. J Oral Maxillofac Pathol 20: 497-504, 2016.
21. Periayah MH, Halim AS and Saad AZ: Mechanism action of platelets and crucial blood coagulation pathways in hemostasis. Int J Hematol Oncol Stem Cell Res 11: 319-327, 2017.
22. Khalele BAEO and Al-Shiaty RA: A novel marker of ameloblastoma and systematic review of immunohistochemical findings. Ann Diagn Pathol 22: 18-24, 2016.
23. Nikitakis NG, Tzerbos F, Triantafyllou K, Papadimas C and Sklavounou A: Granular cell ameloblastoma: An unusual histological subtype report and review of literature. J Oral Maxillofac Res 1: e3, 2011.
24. Zhang YL, Wang RC, Cheng K, Ring BZ and Su L: Roles of Rap1 signaling in tumor cell migration and invasion. Cancer Biol Med 14: 90-99, 2017.
25. Jia Z, Yang Y, Dengyan Z, Chunyang Z, Donglei L, Kai W and Song Z: RAP1B, a DVL2 binding protein, activates Wnt/beta-catenin signaling in esophageal squamous cell carcinoma. Gene 611: 15-20, 2017.
26. Pomin VH and Mulloy B: Glycosaminoglycans and proteoglycans. Pharmaceuticals (Basel) 11: 27, 2018.
27. Hassan N, Greve B, Espinoza-Sánchez NA and Götte M: Cell-surface heparan sulfate proteoglycans as multifunctional integrators of signaling in cancer. Cell Signal 77: 109822, 2021.
28. Winkler J, Abisoye-Ogunniyan A, Metcalf KJ and Werb Z: Concepts of extracellular matrix remodelling in tumour progression and metastasis. Nat Commun 11: 5120, 2020.
29. Listik E, Azevedo Marques Gaschler J, Matias M, Neuppmann Feres MF, Toma L and Raphaelli Nahás-Scocate AC: Proteoglycans and dental biology: the first review. Carbohydr Polym 225: 115199, 2019.
30. Gómez-Herrera Z, Molina-Frechero N, Damián-Matsumura P and Bologna-Molina R: Proteoglycans as potential biomarkers in odontogenic tumors. J Oral Maxillofac Pathol 22: 98-103, 2018.
31. Barkovskaya A, Buffone A Jr, Žídek M and Weaver VM: Proteoglycans as mediators of cancer tissue mechanics. Front Cell Dev Biol 8: 569377, 2020.
32. Yu D, Lim J, Wang X, Liang F and Xiao G: Enhanced construction of gene regulatory networks using hub gene information. BMC Bioinformatics 18: 186, 2017.
33. Li CY, Cai JH, Tsai JJP and Wang CCN: Identification of hub genes associated with development of head and neck squamous cell carcinoma by integrated bioinformatics analysis. Front Oncol 10: 681, 2020.
34. Sun T, Liu Z and Yang Q: The role of ubiquitination and deubiquitination in cancer metabolism. Mol Cancer 19: 146, 2020.
35. Che Z, Sun H, Yao W, Lu B and Han Q: Role of post-translational modifications in regulation of tumor suppressor p53 function. Front Oral Maxillofac Med 2: 1-15, 2020.
36. Zhong M, Li Z, Wang J, Zhang B, Hou L and Gong YB: Expression of telomerase activity and c-myc and stimulatory protein 1 in human ameloblastoma. Hua Xi Kou Qiang Yi Xue Za Zhi 22: 499-502, 2004 (In Chinese).
37. Acosta JC and Gil J: Senescence: A new weapon for cancer therapy. Trends Cell Biol 22: 211-219, 2012.
38. Aebersold R and Mann M: Mass spectrometry-based proteomics. Nature 422: 198-207, 2003.
39. da Silva Marcelino BMR, Parise GK, do Canto AM, Sassi LM, Sarmento DJS, Costa ALF, Hasséus B, Kjeller G, Schussel JL and Braz-Silva PH: Comparison of immunohistochemistry and DNA sequencing for BRAF V600E mutation detection in mandibular ameloblastomas. Appl Immunohistochem Mol Morphol 29: 390-393, 2021.
40. Lapthanasupkul P, Laosuk T, Ruangvejvorachai P, Aittiwarapoj A and Kitkumthorn N: Frequency of BRAF V600E mutation in a group of Thai patients with ameloblastomas. Oral Surg Oral Med Oral Pathol Oral Radiol 132: e180-e185, 2021.